We are IntechOpen, the world's leading publisher of Open Access books Built by scientists, for scientists

4,800
Open access books available

122,000
International authors and editors

135M
Downloads

Our authors are among the

154
Countries delivered to

TOP 1%
most cited scientists

12.2%
Contributors from top 500 universities

WEB OF SCIENCE™

Selection of our books indexed in the Book Citation Index in Web of Science™ Core Collection (BKCI)

Interested in publishing with us?
Contact book.department@intechopen.com

Numbers displayed above are based on latest data collected.
For more information visit www.intechopen.com

12

The Schwann Cell-Axon Link in Normal Condition or Neuro-Degenerative Diseases: An Immunocytochemical Approach

Alejandra Kun[1,2] et al.*
Department of Proteins & Nucleic Acids,
Instituto de Investigaciones Biológicas Clemente Estable (IIBCE), Montevideo, Uruguay

1. Introduction

Peripheral nerve axons of mammals have been demonstrated to contain ribosomes (Court et al., 2008, 2011, Kun et al. 2007, Li et al. 2005a and 2005b, Sotelo et al. 1999), as well as specific mRNAs that have been shown to concentrate in specific peripheral axonal domains (Koenig & Martin 1996, Koenig et al., 2000, Sotelo-Silveira et al., 2006, 2008), the so called Periaxoplasmic-Ribosomal-Plaques (PARPs). Two possible origins have been proposed to supply mRNAs and ribosomes to axons and PARPs: a) from neuronal body axonal transport, or b) Schwann cell to axon trans-cellular transfer (Court et al. 2008, 2011, Sotelo-Silveira et al. 2006, Sotelo et al., to be published elsewhere). We showed that Schwann cell provide newly synthesized RNA (Bromouridine -BrU- labeled RNA) to the axon by a transcellular transfer process. This newly synthesized RNA was provided by Schwann cell nucleus and transported to the axon throughout Schmidt-Lanterman Incisures, and/or Nodes of Ranvier using the actin network, using molecular motors such as Myosin-Va. This was found in normal regenerating nerves disconnected from their neuronal body of origin, meaning that the only possible origin of this axonal RNA is the Schwann cell (to be published elsewhere).

The transfer of mRNAs and ribosomes from Schwann cell to the axon in normal or regenerating nerve fibers we found, make us think about which role it may play in neurodegenerative diseases. Mice models of Charcot-Marie-Tooth (CMT, Trembler-J mouse, Patel 1992, Suter 1992), as well as human nerve samples of CMT patients, were analyzed in

* Gonzalo Rosso[1], Lucía Canclini[1], Mariana Bresque[1], Carlos Romeo[1], Karina Cal[1], Aldo Calliari[1,3], Alicia Hanuz[1], José Roberto Sotelo-Silveira[4,5] and José Roberto Sotelo[1]
1 Department of Proteins & Nucleic Acids, Instituto de Investigaciones Biológicas Clemente Estable (IIBCE), Montevideo, Uruguay
2 Biochemical Section, School of Science, Universidad de la República (UdelaR), Montevideo, CSIC Project, UdelaR, Uruguay
3 Biophysics Area, School of Veterinary, (UdelaR), Montevideo, Uruguay
4 Cell and Molecular Biology Department, School of Sciences, (UdelaR), Montevideo, Uruguay
5 Department of Genetics, Instituto de Investigaciones Biológicas Clemente Estable (IIBCE), Montevideo, Uruguay

order to study the metabolic characteristics of this Schwann cell-axon relationship may have to the pathogenesis of this important human illness.

CMT is the most frequent genetic peripheral neuropathy (1/2500 prevalence, Berciano & Combarros, 2003, Inherited Peripheral Neuropathies Mutation Database: www.molgen.ua.ac.be/cmtmutations). This chronic progressive illness has two possible origins: axonal, CMT-II (neurofilament, KIF 1B or Rab7 protein mutations, among others), or Schwann cell, CMT-I (PMP-22, Conexin 32, P0 protein mutations, among others, Mersiyanova et al, 2000, Pérez-Ollé et al, 2002, Verhoeven et al, 2003, Zhao et al, 2001). Regardless the initial alteration, all CMT end in a functional axonopathy, which emphasize the importance of Schwann cell-axon relationship in the context of the gene expression of both cells. This local supply of transcripts may be altered in CMT, probably causing the final pathologic phenotype.

The histological analysis of CMT (I or II) patients' nerves showed the conventional myelin or axonal typical alterations (onion bulbs, axonal ovoids, internode shortening, fiber diameter variations, paranodal remyelination, etc.), plus a marked increase of axonal sprouting (myelinopathies). Molecular composition of CMT1 human patients, normal rats, PMP-22 mutant mice nerves, as well as mice organotypic dorsal root ganglia culture, was characterized here. More and more, mutant animals, transgenic animals, transfected cell culture, or cell culture obtained from any of these animal types are used to unravel the pathogenesis of important human diseases. The present paper contribute to the understanding of human Charcot-Marie-Tooth syndrome, because as we will describe below we found abnormal distribution of mutant PMP-22 transcript and protein, but also an irregular accumulation of ribosomes on altered Schwann cells and axons.

2. Schwann cell organization. Characterization of normal human and rat Schmidt Lanterman Incisures (SLI)

Whole mount of normal teased human and rat peripheral nerve fibers preparation let us know the normal interrelation between glia cell and axons in PNS. Teased fibers of Human Sural nerves and rat Sciatic nerves, (immunostained by floating), permitted to characterize the molecular expression of both nerve cells, Schwann cell and neuron (axonal domain). Internodal non-compact myelin mainly represented by Schmidt Lanterman Incisures (SLI) has been clearly characterized in this type of whole mount. Confocal single stacks show the SLI immunoreactivity with antibodies against tubulin, vimentin, Myelin Associated Glycoprotein (MAG) and ribosomes, in human sural nerve teased fibers (arrows in Figure 1, A green, B, C and F, respectively). Ribosomes are present in Schwann cell cytoplasm, Nodes of Ranvier and SLI (Figure 1, F). Nucleic acids have been also found in SLI of human fibers, identified by a fluorescent specific probe (Yoyo-1) as can be seen in Figure 1 D. Central axonal area in human longitudinal fiber appear strongly stained with anti-Neurofilament-200kDa (Figure 1, E,). Vimentin seems most evident in external Schwann cell and SLI cytoplasm (Figure 1, C). Filamentous actin, recognized by Phalloidin coupled to Alexa 546, shows a moderate signal in Schwann cell cytoplasm and axoplasm, and a more vigorous signal in SLI (Figure 1, A red). A similar signal pattern has been seen in rat sciatic teased fibers (Figure 1, J, K, L). A three dimensional reconstruction of confocal stacks series from a whole mount single fiber (rat), immunostained with anti-ribosomal antibody, let as to identify the spiral funnel-like path of

SLI. The whole reconstruction was 90º rotated to show the SLI image (Figure 1, M), enreached in ribosomes. The same SLI path image is outlined in Figure 1, N. The fine structure of myelinated sural human fibers show a well organized SLI (Figure 1 H, clear arrow). The compact myelin (Figure 1 H, white asterisk), surround the non compact myelin of SLI (Figure 1, H clear arrow). The external SLI domain is characterized by a well structured autotypical adherents type junction (Figure 1, H asterisk). Near this region, it can be seen the external mesaxón (Figure 1, H, black arrow). The external Schwann cell cytoplasm (Figure 1, H, eSc) appear clear, with evident cytoskeleton. Boxed area in H is enlarged in I. Close to the axolema, Schwann cell cytoplasm among the non compact myelin membranes of the SLI (Figure 1, I, asterisk), show the presence of a Multivesicular Body (Figure 1, I arrow). Near this region, the compact myelin, appear devoid of cytoplasm. Internodal regions constitute the largest domain of contact between the glial cell and axon. However, the molecular characterization of internodal transcellular interactions is barely known. Non-compact myelin is found in paranodal regions and Schmidt-Lanterman Incisures, which traverse diagonally compact myelin. It is postulated that, under normal conditions, the presence of cytoplasm in SLI would ensure protein turnover and vesicular trafficking (lysosomes, vesicles of endoplasmic reticulum) for the homeostasis of essential myelin and cell domains distant within the glial cell itself. These glial "shortcut" have been largely described in literature. The internodes SLI's number varies, depending on the species, axonal diameter and physiological conditions (Cajal, 1928, Ghabriel, et al., 1979a and b, 1980a and b, 1981, 1987; Hiscoe, 1947; MacKenzie et al., 1984; Robertson, 1958,). In the present work SLI have been characterized throughout the molecular expression of cytoskeleton components (actin, tubulin, vimentin) and adhesion molecules (MAG), showing that the SLI cytoplasm have well organized "roads" devoted to traffic. The presence of multi-vesicular bodies at the SLI have been seen in the past (Hall &Williams, 1970) as has been also described here, revealing an active vesicular metabolism in the cytoplasm of non compact internodal myelin. The expression of nucleic acid especially ribosomal RNA, indicate that SLI and Nodes of Ranvier have local traffic of translational machinery. Why ribosomes could be transported to these domains? One of the possible answer is the local synthesis of glial and myelin proteins. However, we noted other possible roles related to axon-glia homeostasis and axonal maintenance (Court et al., 2008; Kun et al., 2007, Sotelo-Silveira et al., 2006), which could be altered in pathological conditions. Some of our more recent results contribute to this hypothesis. Indeed, we found a SLI local expression of heavy neurofilament subunit mRNA and his final product, the corresponding protein, in normal and pathological conditions (manuscript en redaction). However it is important to highlight that trans-cellular traffic between Schwann cell and axon especially through SLI implies vesicular transport system inside SLI and a trans-endocytosis mechanism between both nerve cells. That would mean a different set of adhesion and signaling molecules in each part of this process, where MAG seems to be one of the candidates molecules involved. MAG expression is specific to myelin-forming cells in the early process of myelination. One of its functions is to promote initial interactions in the process of fastening the first layer of myelin around axons (inner mesaxon), and further development of myelin. But the level expression of MAG is relatively high, suggesting other possible roles. Among them, a particularly important role for MAG is the receptor binding axonal ligand (protein-ganglioside complex), which could activate intra-axonal signal transduction cascades necessary for the maintenance and survival of myelinated axons (Quarles, 2007).

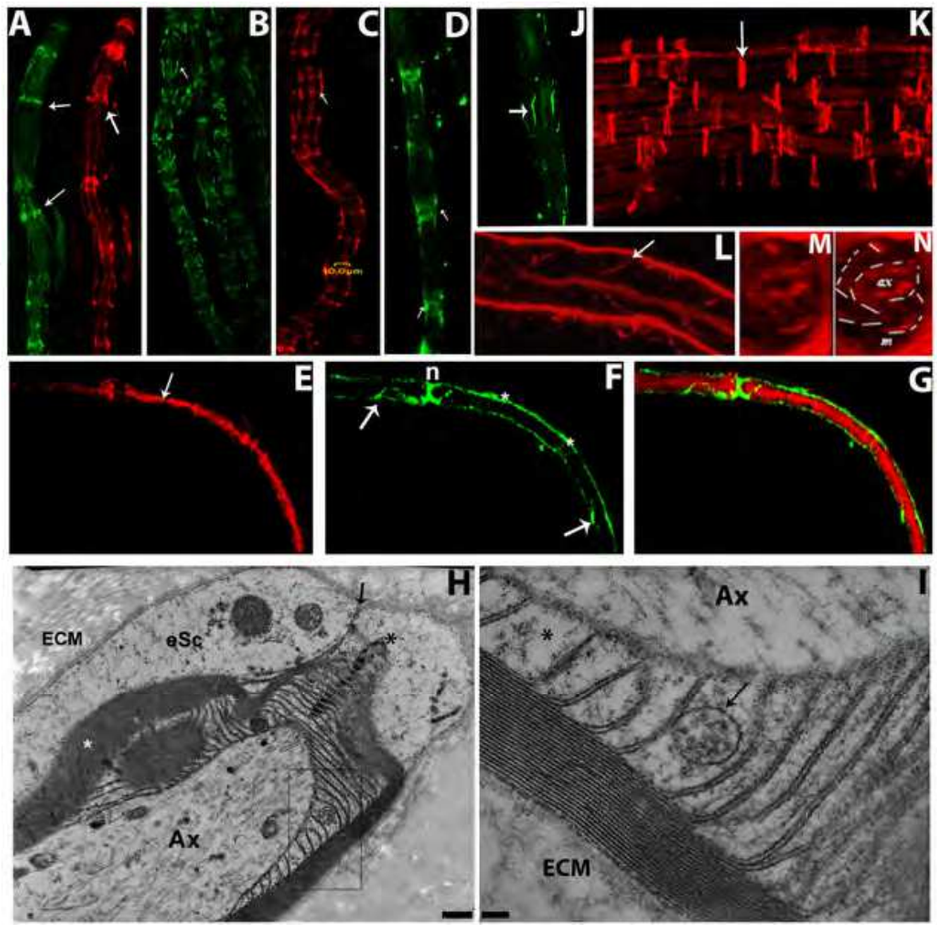

Fig. 1. Molecular characterization of normal Schmidt Lanterman Incisures (SLI) and Nodes of Ranvier (NR), in human and rat peripheral fibers.

Human SLI have been studied by immuno-confocal microscopy (A-G) and conventional electron microscopy (H and I). Human sural teased fibers were immunostained and observed by confocal microscopy. Single confocal planes show SLI (arrows) enriched in Myelin Associated Glycoprotein (A, green), Actin (A, red), Tubulin (B) Vimentin (C) and nucleic acid (D, Yoyo-1) and a few NR. Among them, the ribosomes (F, green) are present in Schwann cell cytoplasm (asterisk), in Nodes of Ranvier (F, n) and SLI (arrows). Central axonal domain appear strongly stained with anti-Neurofilament -200 kDa (E in red, arrow), merged image is shown in G showing how ribosomes are entering to the axon throughout NR (demonstraded by Z stacks analysis, not shown here) and SLI. Actin (K, in red), nucleic acids (J, YoYo-1, in green) and ribosomes (L in red) are also present in SLI of rat sciatic teased fibers. Three dimensional reconstruction of panel L, in which Z-stacks series was rotated 90º to show the SLI funnel spiral path image in M, enriched in ribosomes. The SLI path is outlined, in the same image, in N (ax, axoplasm; m, myelin). TEM, the ultrastructure of semi-longitudinal section of human sural fiber reveal a well organized SLI (H, clear arrow). In H, black asterisk shows the external part of SLI adherens junction, black arrow indicates the external mesaxon and white asterisk indicate compact myelin. The external Schwann cell cytoplasm (H, eSc) and the extra cellular matrix (H, ECM) are also indicated. Boxed area in H is enlarged in I. The presence of

Schwann cell cytoplasm among the non compact myelin membranes of the SLI (I, asterisk) might be observed, meanwhile it is completely absent in adjacent compact myelin. A Multivesicular Body (MVB) is present in the SLI cytoplasm (I, arrow). Bar in H represents 400nm, bar in I represents 100nm.

3. Schwann cell and axonal ribosomes have been identified in normal rat sciatic nerve fibers. Post-embedding immuno-gold staining

Normal rat sciatic nerve fibers have been explored to highlight the distribution of translational machinery, based on ribosomal recognition. An expected pattern of Schwann cell ribosomes (internal positive control) has been found by indirect postembedding immunogold staining (Figure 2, B), where it is possible to recognize immunocomplex in Schwann cell cytoplasm (Figure 2, B, box 8) and in myelinic region (Figure 2, B, boxes 8 and 9). Immunocomplex, recognized by gold particles are also present in the axoplasmic domains (Figure 2, A and B, box 10). Axoplasmic immunogold complexes (Figure 2, A, box 1) have a diverse distribution involving mitochondria (Figure 2, A, M) and their proximity (Figure 2, A, box 6). The immunocomplex seems to be associated to the cytoskeleton (Figure 2, A, boxes 2, 4 and 6), or in a multivesicular like-body (Figure 2, A, box 5). Axoplasmic polysomes not associated to cytoskeleton, has been found linked to immunogold particles (Figure 2, A, box 3). The samples were not osmificated previously to LRW inclusion, but exposed to osmium vapor, after immunostaining. Because that, the membranes are poorly countersained in LRW. The ultrathin sections were incubated with uranyl acetate and lead citrate as usual in Transmission Electron Microscocopy (TEM).The uranyl solution recognize the amino and phosphate groups of proteins and nucleic acid, while lead citrate is osmium-enhancing and bind to hydroxyl groups (also including phosphate groups). The absence of osmium staining before the inclusion, also result in a weak lead salt counterstaining. The Nano-gold particles have 15 nm in diameter.

TEM experimental evidences have demonstrated the presence of ribosomes in normal peripheral axons in different species including invertebrates (Kun et al., 1998 and 2007; Koenig and Martin, 1996; Zelena, 1972a, 1972b and 1970; Martin et al., 1989; Sotelo et al, 1999;). Axonal translational machinery could play an important role in structural and physiological maintenance, especially considering renewal and turn-over of proteins. Considering the Schwann cell as a positive internal control (as well as mitochondria, since the polyclonal antibody recognized also prokaryotic ribosomes), comparing their ribosome immunoreactions, axonal ribosomes appear associated to cytoskeleton in free polysomes-like complex. We have proposed that the axoplasmic ribosomes could have two possibles origins: the neuronal cell body and the neighbor Schwann cell (Kun et al. 2007; Sotelo-Silveira et al., 2006,). Peripheral normal axons run unusual long distances in cellular scale. However, its unusual geometry does not affect the homogeneity of the axoplasm. Cajal (1928), proposed that Wallerian degeneration was somehow in equilibrium with axon regeneration, and now we know that the axon is a dynamic steady state. Meanwhile, in hereditary peripheral neurodegenerative diseases (CMT, the most frequent peripheral human neuropathy), there is a chronic condition where the "normal" equilibrium is never reached. In addition, the chronic condition makes the displacement of the equilibrium always worst, because cellular repair mechanisms are insufficient to reverse the illness progress. In those conditions, the repair mechanisms are permanently activated. The resultant neuro-pathological phenotype, as occur with the normal phenotype, emerges from the integration of both Schwann cell and the axons (Aguayo et al, 1977; Salzer et al., 2008; Suter and Scherer, 2003,).

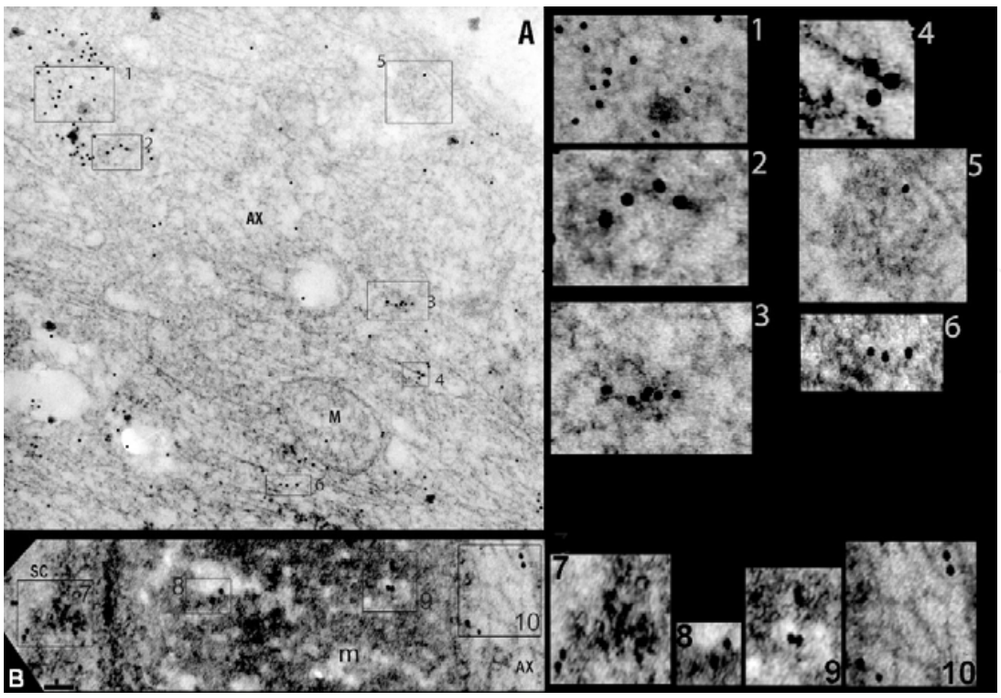

Fig. 2. TEM, normal rat sciatic nerve, postembedding ribosome immuno-gold staining.

Ultrathin transversal sections of rat sciatic nerve included in LRW hydrophilic resin was immunostained using a specific polyclonal antibody against ribosomes (raised in rabbit Kun et al. 2007), recognized in time by a goat-antirabbit gold conjugated antibody. It can be observed in A the presence of single or grouped axoplasmic immunocomplex, recognized by gold particles. The immunocomplex are framed in different boxes (boxes 1, 2, 3, 4, 5 and 6), some close to mitochondria (box 6) and within it (M, mitochondria), associated to the cytoskeleton (boxes 2, 4, 5 and 6), or in a Multivesicular like-Body (box 5). The polysomes domain are clearly decorated by immunogold particles (box 3).The boxed areas in A are enlarged in numbered boxes on the right hand (1 to 6). Different transversal fiber domains show immunogold staining (B, box 7, 8, 9 and 10). The material was included without conventional posfixation or staining in block (osmium tetroxide, uranil acetate). After imunostaining, the ultrathin sections were exposed to osmium vapors (to specially emphasize the membrane structure) and counterstained with uranyl acetate and lead citrate as usually used in TEM. The bar in A and B represent 100nm, each gold particle has 15nm in diameter. AX, axoplasm; M, mitochondria; m, myelin; SCc, Schwann cell cytoplasm.

4. Schwann cells' ribosomes are involved in axonal sprouting of human CMT-1 sural nerve fibers. Axonal sprouting is promoted by myelin compaction decrease

The presence of ribosomes has been used to recognize the Schwann cell citoplasmic domains in CMT-1 human patient whole mount of sural nerve teased fibers, immunostained by floating. A longitudinal confocal tridimensional reconstruction of one of that fibers is showed in Figure 3, A and B (original image is showed in A, but specific cellular domains have been outlined in B). Delaminated myelin (dM) let the Schwann cell

cytoplasm (Figure 3, B, SCc) expand among their de-compacted layers, that appears strongly stained with ribosomes (Figure 3 A and B, red signal). Some of the ribosomal signals are also present at the axoplamic region (Figure 3B, merged yellow, asterisks) in the main axon (Figure 3 B, mAx) and in the origin of the new-born axon-sprout 1 (Figure 3B, oS1). Next to the main axon, a bulk of ribosomes also surround axonal sprouting path (Figure 3B, R). The axonal domains are identified by phosphorylated neurofilament protein (NF-P) signal (Figure 3, green). An inhomogeneous arrangement of NF-P signal distribution (characteristic of this pathology) is showed in the main axon (Figure 3B, mAx) and in the lateral sprout axons 1 and parallel axon sprout 2 and 3 (Figure 3 B, S1, S2 and S3). A similar pattern of expression is showed in other single human CMT-1 sural teased fiber showed in Figure 3 C, D and E. A most homogeneous distribution of NF-P signal is observed in that fiber. The main axon and their sprouting, NF-P signaled (Figure 3 C, green), also expand among the delaminated myelin, highly decorated by ribosomes (Figure 3 D, red signal). It is a longitudinal image of a conventional "onion bulb" typical diagnosis image, with specific molecule expression.

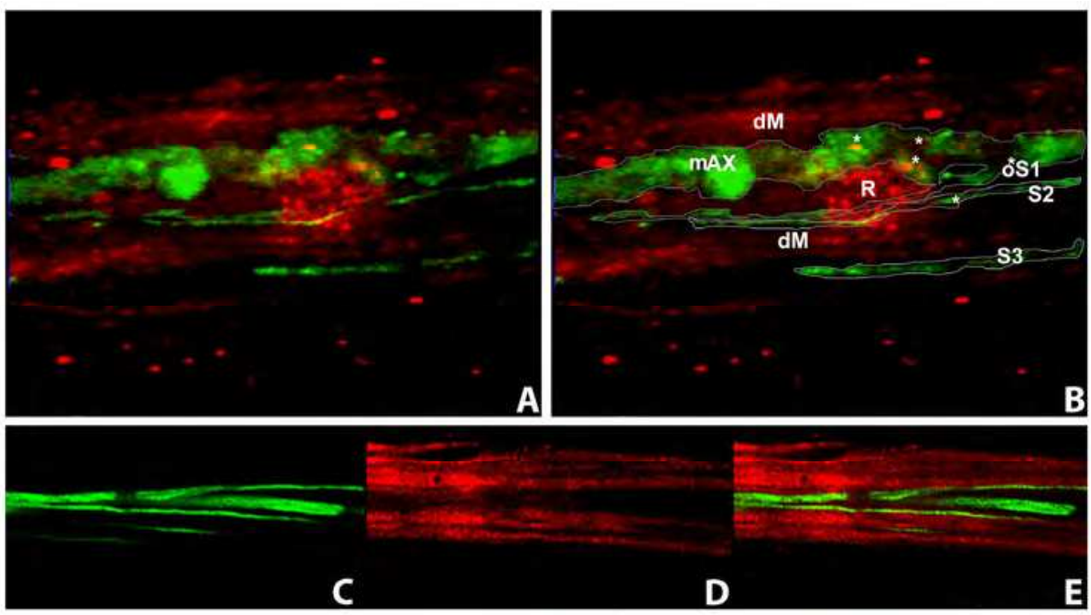

Fig. 3. Ribosomes and Phosphorylated Neurofilaments in Human CMT-1 sural teassed fiber. A. The original image is shown in A, while the specific cellular domains and components have been outlined and indicated in B. The image show a longitudinal single teased fiber from a human CMT1 sural nerve (confocal tridimensional reconstruction). The main axon (mAx) shows an inhomogeneous distribution of phosphorylated neurofilaments (green) and a lateral axoplasmic sprouting (S1) originated from the main axon (oS1). The delaminated myelin (dM) allows the Schwann cell cytoplasm (SCc) to expand among their membranes strongly inmunostained by the ribosomal antibody (red). The presence of ribosomes are also evident at the axoplasmic level (asterisks, merged color) in the main axoplasm and in the new-born axoplasm (sprouting, S1). A big conglomerate of ribosomes (R) appears close to the main axoplasm and it is crossed by the (S1). Sproutings running in parallel to the main axon can be also seen in the same image (S2, S3). A human teased sural fiber from other

CMT1 patient is showed in C, D and E. The axoplasm is also identified by the phosphorylated neurofilament (green, C) and the Schwann cell cytoplasm by the ribosomes (red, D). The image shows a longitudinal "onion bulb"-like organization (E, merged image). Also are evident the thin sprouts originated from the main axon, passing throughout the layers of delaminated myelin.

Alteration in PMP-22 represent 70% of myelinopathy (Young et al., 2003), in demyelinating human peripheral fibers, we observed axonal sprouting consequently with the lack of inhibitory effect of myelin and normal Schwann cell (Shen et al., 1998; De Bellard et al., 1996). This axonal growing is in close relation with structural and functional changes, as observed among myelin disassembly, axonal sprouting. Trembler-J mice (*Tr-J*) develop a neurodegenerative phenotype that is validated as an animal model of CMT1A (Devaux and Scherer, 2005; Sereda and Nave, 2006; Sidman et al, 1979). Gene mapping indicates that the primary defect is a mutation resulting in a leucine (16) to proline substitution in PMP-22 (Suter et al, 1992). The same amino acid substitution was found in a human family who suffered CMT1A (Valentijn et al, 1992). This substitution prevents normal protein folding, insertion into the membrane and normal myelination. Heterozygous mice (Trj/+) show a spastic paralysis and generalized tremor. While homozygous mice (TrJ/TrJ), show more severe peripheral myelin deficiency, causing death before weaning (Henry et al, 1983; Henry and Sidman, 1983; Suter et al, 1992). The main changes affecting the SNP, begins to be evident from post-natal day 20 (P20), showing a characteristic body tremor and the impossibility of abduction and extension of the hind legs (from P11), as we recently described (Rosso et al, 2010). Typically the mutation is confirmed by individual genotyping of mice (mainly by PCR-RFLP; Notterpek et al, 1997; Fortun et al, 2005; Khajavi et al, 2007, Rosso et al, 2010).

5. Schwann cell express a mutate pmp22 gen in CMT-1A animal model (Trembler mouse). Peripheral Myelin Protein-22 in vitro distribution is altered in Trembler J mice

The PMP-22 is a myelin protein whose mutation is characteristic of CMT1A human peripheral illness. Trembler J mice is an animal model to study CMT1A caused by *pmp22* mutation. The Schwann cell expression of *pmp22* (green) has been observed in normal (Figure 4, WT, A and B) and heterozygous (Figure 4, TrJ, D and E) organotypic culture of embryonic dorsal root ganglion (DRG). The wild type (WT, +/+) Schwann cell *pmp22* RNA is observed at cytoplasm and in perinuclear domains, excluding the nucleoplasm, that appear mostly empty of ISH signal (Figure 4, asterisk in A and B). The opposite is observed in Trembler J heterozygous (HZ, TrJ/+) DRG, where the *pmp22* expression is mostly concentrated into nuclear and perinuclear domains (Figure 4, asterisk in D and E). When the PMP-22 expression was analyzed in adult sciatic nerves, the immunocytochemical signal also appears concentrated in the nucleoplasm of HZ teased fibers (Figure 4F, green, asterisk). The adult WT teased sciatic fibers showed a cytoplasmic and perinuclear distribution, excluding the nucleoplasm (Figure 4C). Axoplasmic and Schwann cell domains are also counter stained with anti NF-68 antibody (blue signal) and Phalloidin-Alexa 546 (red signal) in Figure 4, C and F. In TrJ/+ mice the whole expression of *pmp22* is concentrated at Schwann cell nuclei region (Figure 4D, 4E and 4F).

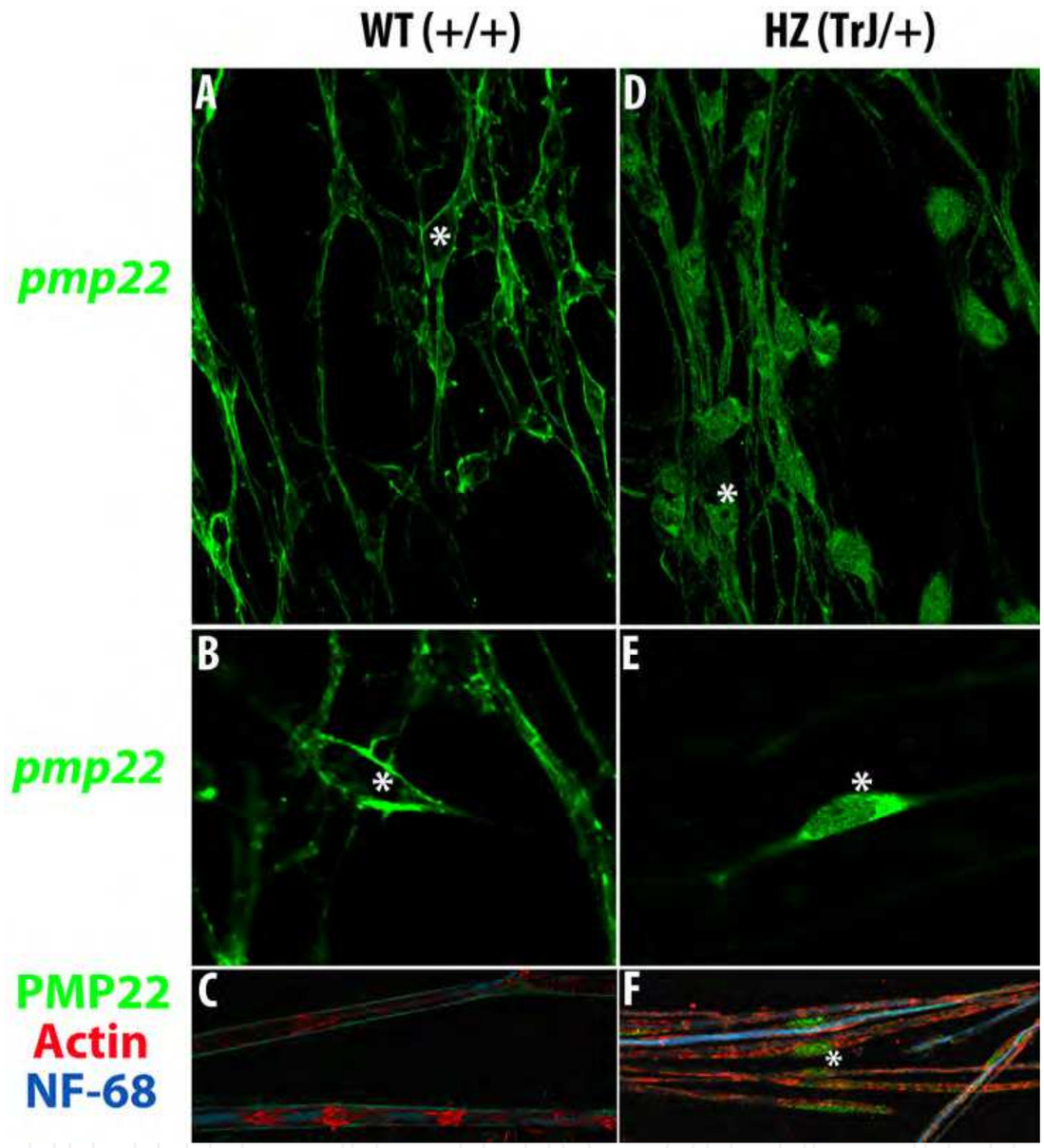

Fig. 4. Peripheral *pmp22* expression. The expression of peripheral myelin proteín 22 gene might be observed in normal (WT, +/+, A and B) and heterozygous (HZ TrJ/+, D and E) cultured E13 DRGs. In normal genotype (+/+), the Schwann cell transcript distribution show a peri-nuclear cytoplasmic arrangement, remaining the nucleoplasm almost empty of In Situ Hybridization (ISH) signal (asterisk in A and B); meanwhile in the Schwann cell from mutants (TrJ/+), the whole nuclear domain appear filled of *pmp22* ISH signal (asterisk in D and E). B and E are different regions at higher magnification. C and F show immunocytochemical recognition of proteins: PMP-22 (green), Actin (red) and Neurofilament 68kDa subunit (blue) in WT +/+ (C) and HZ TrJ/+ (F) in teased sciatic nerve fibers from adult mice. As we showed for *pmp22* transcript the mutant HZ TrJ/+ Schwann cell nuclei not only contain the RNA, but the product of its translation PMP-22 protein (F, green). The opposite occurs in WT (A, B and C).

In myelinating Schwann cells from adult Trembler-J mice, PMP-22 protein accumulates in cytoplasmic aggregates, ER-Golgi compartments and is associated with other proteins in endosomes and lysosomes suggesting high levels of protein degradation (Suter and Snipes, 1995a, 1995b). In normal Schwann cells, ~80% of the newly-synthesized PMP-22 is degraded within 30 min by the proteasome, likely due to inefficient folding (Notterpek et al 1999a; Ryan et al., 2002). The proteasome is a multi-catalytic complex involved in a variety of cellular processes, including the degradation of short-lived proteins (Goldberg, 2003). PMP-22 is a short-live molecule, that form aggregates when the proteasome is inhibited or the protein is mutated (Fortun et al., 2007). It is conceivable that the amount of PMP-22 targeted for degradation is increased in the gene duplication and point mutations disease, which could overwhelm the proteasome and lead to the accumulation of miss-folded proteins along the secretory pathway. Removal of pre-existing PMP-22 aggregates is assisted by autophagy, and chaperones/autopaghy induction can suppress accumulation of PMP-22 aggregates. The expression of *pmp22*, observed in WT (+/+) DRG cultures, occurs from early stages of culture, showing a discrete distribution in any glia cytoplasm, including perinuclear region, correlating strongly with PMP-22 expression (data not shown). Adjacent axons show the presence of phosphorylated neurofilament, typically with discontinuous distribution (data not shown). However, in HZ (TrJ/+) DRGs, the *pmp22* distribution is concentrated almost exclusively in glial nuclear and perinuclear regions, being absent from the glial myelin domains along the axon. In adults TrJ/+ fibers the nuclear and perinuclear PMP-22 expression confirm a pattern of mutated *pmp22* expression conserved from early myelination to adult stage. PMP-22 signals are granular and form a bulk of molecules, similars to those described as aggresomes. It has been described that aggresome formation is accompanied by redistribution of cytoskeleton components. Intermediate filaments, play key role forming a condense cage surrounding a pericentriolar aggregated and ubiquitinated proteins. A growing number of disease-associated proteins have been found to accumulate in aggresomes, including peripheral myelin protein 22 (PMP-22) (Notterpek et al., 1999; Ryan et al., 2002), huntingtin (Waelter et al., 2001), parkin, and alpha-synuclein (Junn et al., 2002). However, the presence of *pmp22* transcript and PMP-22 protein signals in nuclear domains during myelinogenesis and in TrJ/+ adult fibers, respectively (Fig. 4), suggest other type of alterations. Would they be, a) an altered post-transcriptional regulation, and/or b) an altered motor protein link, potentially involved in pathogenesis and illness consolidation.

6. Experimental procedures

6.1 Animal care and maintenance

Rattus norvegicus (Sprague Dawley) were obtained from the IIBCE colony. TremblerJ (B6. D2-Pmp22 <Tr-j>/J, Jackson Laboratory, USA) mice colony was started in 2008 (CSIC Grant-Universidad de la República 2005-2009). These mice carries a spontaneous mutation in Peripheral Myelin Protein-22 (PMP-22). All mice are recorded, numbered and genotyped following the method previously described (Rosso et al, 2010). Harems are formed after determining the stage of the female estral cycle. Pregnancy starts is determined by the examination of vaginal exudates and controlled by weekly weight of females. The colony, have now 100 animals, living in isolated cages, stored in isolated rooms.

All animals are maintained under controlled temperature and light cycle. Water and food are supplied *ad libitum*. The animal housing conditions are in agreement with the National

Committee for Animal Care and Maintenance (CHEA-Universidad de la República-Uruguay, *www.chea.udelar.edu.uy*)

6.2 Trembler J mice genotyping

Genomic DNA was extracted using a phenol–chloroform based method. DNA concentration was determined by spectrophotometry. PCR was performed on 200ng of DNA using specific primers (forward: 5′-GTTCCAAAGGCAAAAGATGTTC-3′; reverse: 5′-AACAATAAT CCCAAACCACACTTC-3′) that flanked the mutation site. PCR products were digested with BfaI (Fermentas) for 2h at 37 ◦C and separated by 6% polyacrylamide gel electrophoresis (PAGE). The digestion products were stained with AgNO3. The BfaI digestion of the amplified fragment from the wild-type allele produced two fragments of 221 and 500 basepairs (bp).The TrJ mutation results in a loss of the BfaI site. Consequently, the amplified fragment obtained using the TrJ allele as template was visualized as a single band of 721bp**.**

6.3 DRGs organotypic culture

Thirteen day mice embryos (E-13) were euthanized and Dorsal Root Ganglia were collected for organotypic culture in appropriated media (Neurobasal (Invitrogen) complemented by 0,20 ml/ml B27, 0,01µg/ml Nerve Growth Factor (NGF) and 2mM glutamax). The culture was done at 37ºC under 5% CO_2 controlled atmosphere. The cultured medium was changed every 48 hours. At 16 days of dorsal root ganglia culture, the culture media was complemented with 50µg/ml Ascorbic Acid, to promote *in vitro* myelination.

6.4 Fixation

Rats and mice were euthanized under pentobarbital anesthesia following the Uruguayan Committee for Ethical Animal Experimentation (CHEA in Spanish). Rats were euthanized by intracardiac perfusion of fixative (4% paraformaldehyde (PFA) for confocal microscopy and 0.25% glutaraldehyde was added for Electron Microscopy (EM) in PHEM (25mM HEPES, 10 mM EGTA, 60 mM PIPES, 2mM MgCl2 , adjusted to pH 7,2- 7,6, with KOH) after heparinization. Sciatic nerves were excised immediately after perfusion (cut in 2-mm pieces), pre-immersed in the same fixative solution for 2 hr, then washed in PHEM for 2 hr (gentle stirring), changing solution every 10 min. Mice sciatic nerves were excized and fixed by immersion in 3% PFA in PHEM, 30 minutes, at 4ºC. The samples were then washed 6X5 minutes with gentle stirring. Cultured ganglia were fixed by 10 min immersion in 2% PFA in PHEM. Throughly washed in PHEM 1 hour (6 X 10 min). The samples followed different pre-treatement before in situ molecular studies.

6.5 Human samples

Clinically diagnosed patients with a family history of polyneuropathy, presenting a chronic sensory-motor polyneuropathy were included in the present study. Electrophysiological studies were performed to confirm the nature of the demyelinating neuropathy prior to their inclusion. Alcoholics, diabetics, exposed to toxic or neurotoxic drugs and/or bearers of

systemic diseases patients were specifically excluded. Electrophysiological studies were: nerve conduction velocity analysis, electromyogram and quantification of motor units. Patients meeting the inclusion criteria have been informed of the study and samples were taken only after they signed an Informed Consent to participate in the CSIC I+D (2005-2009) Project (Grant from Universidad de la República, Uruguay). Human control was obtained from Human whole donors from the "Instituto Nacional de Donantes y Trasplantes de células, Tejidos y Organos (INDT)". Briefly, a portion of each sural nerve biopsy from human CMT patient, used for histopathological diagnosis was fixed in 3% PFA diluted in PHEM, 30 minutes at 4ºC with stirring. Fixative was washed with PHEM (6X10 minutes). When it was possible, the epineuria was removed to facilitate the ulterior treatments.

6.6 Electron Microscopy

Nerves pieces were processed for postembedding immunostaining. (Bozzola & Russel, 1998; Vazquez Nin, 2001). Briefly, nerve pieces were dehydrated increasing concentration of alcohol, until pure alcohol. Thereafter were embedded in hydrophilic resine LR-white (LRW) by increasing its concentration. When they were in pure LRW (overnight at room temperature), the blocks were polymerized, under anhydrous conditions, in two steps: 24 hs at 45ºC and 24 hours at 60ºC. Ultrathin sections (60-100 nm) were obtained by ultramicrotomy and collected in nickel grids, without film. Indirect immunostaining was followed. The grids were placed exposing the ultrathin section to different series of drops on Parafilm extended layer. The general processes are described under "*Immunostaining*". After that, sections were exposed to Osmium Tetroxide vapours and counterstained with Uranyl Acetate and Lead Citrate as usual in Transmission Electron Microscopy (TEM).

7. Immunocytochemistry

7.1 Pre treatment

7.1.1 Collagen digestion

Epineuria from intact nerve mice were dissected and the extracellular matrix was unstructured by collagenase digestion with Collagenase XII (Sigma), 0.3mg/ml dissolved in PHEM without EGTA (25mM HEPES, 60 mM PIPES, MgCl2, pH 7,2- 7,6) with 5mM CaCl2 final concentration, 1 hour, at 37ºC. The enzymatic activity was stopped by cold washing in buffer PHEM (3X10 minutes).

7.1.2 Teasing

After collagenase digestion, rat and mouse sciatic nerves were placed on a cold slide and were mechanically teased under stereoscopic microscope using blunt needles to prevent fibers tearing. Further treatments were performed over floating fibers.

7.1.3 Resin relaxing

Ultrathin LRW sections were incubated 10 minutes in sodium periodate 0.56M in water at room temperature (RT) to relaxing the resin and washed thereafter with PHEM (6X5 minutes), to remove resins.

7.1.4 Permeabilization

The permeabilization must be a single event that will balance the benefit of increased accessibility of intracellular epitopes for immunocytochemistry or ISH with the hindrance of the consequent deterioration of the structure to be recognized. Cell membranes were permeabilized once with Triton X-100 0.1% in PHEM, at variable times (10 minutes for cell cultures to 30 minutes for whole fibers and LRW ultrathin sections), stirring at RT. Excess detergent was removed by successive washes in buffer PHEM (3x5 minutes). In the procedures that follows no detergent was used. No detergent was used in human samples.

7.1.5 Aldehyde blocking

To reduce background from aldehydes and ketones free groups (generated by fixative or belonging to the cellular structure) they were blocked by incubation with sodium borohydride 0.1% in water for 10 minutes (in cell cultures) or 20 minutes (in intact nerve), at RT. The remains of borohydride are eliminated by repeated washings with buffer PHEM at RT and gentle stirring.

7.1.6 Unspecific antigen blocking

In indirect immunostaining, nonspecific antigen reactions were blocked using 5% normal serum from the animal species in which the anti antibody was raised, dissolved in incubation buffer (IB, 0.150 mM glycine, 0.1% Bovine Serum Albumin in PHEM), 30 minutes at 37°C. After that, the tissue or cells were immediately incubated with the specific antibody.

7.1.7 Immunostaining

After pre-treatment, the procedure was done basically as described by Kun et al (2007) and Sotelo et al. (1999), with some modifications. The sections were incubated 1 h at 37ºC with the specific antibodies in IB (see above) in a wet chamber. Washed 3X5 min, at 37ºC with IB and incubated over 45 minutres at 37ºC with the anti-antibodies. Fluorophores photobleaching was avoided maintaining the slices in dark. The non binding antibodies were eliminated by washing with IB (3X5 min) at 37ºC and PHEM (3X5 minutes) at RT. Slides for confocal microscopy were mounted with Prolong Gold Antifade (Invitrogen). The ultrathin sections were counter-stained as described in "*Electron Microscopy Section*".

7.1.8 Specific antibodies and fluorescent probes

The specific antibodies used in the present work, were: polyclonal anti-Ribosomes antibody (Kun et al, 2007) work dilution 1:500, monoclonal anti phosphorylated Neurofilament (Stemberger) work dilution 1:2500; monoclonal anti-Neurofilament-200 (phosphorylated and non phosphorylated) from Sigma, working dilution 1:800. Human anti-P ribosomal protein (Immunovision) working dilution 1:100, polyclonal anti-Myelin Associated Glycoprotein S/L (MAG, Chemicon) working dilution 1:150; monoclonal anti-Vimentin (Sigma) working dilution 1:400; Alexa-546 Phaloidin (Invitrogen) working dilution 1:40. YoYo-1 (Invitrogen) 1:1000; DAPI (Sigma) working dilution 1:1000.

7.1.9 Secondary-antibodies

The anti-antibodies used in the present work were: Goat anti-Mouse Alexa 488 (A11029, Invitrogen), working dilution 1:2000, Goat anti Rabbit Alexa 546 (A11030, Invitrogen), working dilution 1:2000, Goat anti-Mouse CY5 (Chemicon) working dilution 1:800; Goat anti-Rabbit 15nm gold conjugated (Aurion) working dilution 1:80.

7.2 *In situ* hybridization

The cDNA encoding mouse *pmp-22* mRNA region (425-538) was cloned in the PST-19 plasmid. The plasmid was linearized with HindIII or EcoRI and used as template by *in vitro* transcription reactions. Single-stranded RNA probes were transcribed using SP6 or T7 RNA polymerase according to manufacturer's instructions and labeled with digoxigenin-UTP (Roche). The samples were first permeabilized as indicated in "Permeabilization Section". The endogenous peroxidase was blocked with 0.03% H_2O_2 diluted in PHEM during 1 hour at RT, changing the solution every 15 minutes to refresh the offer of hydrogen peroxide. The samples were then washed with PHEM (3X5 min). The pre-hybridization condition was performed to avoid unspecific probe binding. The prehybridization and hybridization was done in the same condition: incubation with hybridization solution (10% dextran sulfate, 0.1mg/ml tRNA, 0.5mg/ml salmon sperm DNA, 50% formamide, 4XSSC) during two hours at 50ºC without probes (prehybridization) or with sense/antisense probes. Immediately before hybridization, digoxigenin labeled transcripts were denatured 3 min at 95ºC and fast returning to 4ºC thereafter; 5 min to denature the RNA, avoiding the RNA folding. The non hybridized RNA probes were eliminated by repeated washing with decreasing saline concentration (stringency increase), until 0,25X SSC. After that, the hybrid was fixed with fresh prepared 2% PFA in PHEM and gently washed with PHEM (3X5minutes). The hybrid was recognized by sheep anti-digoxigenin antibody conjugated to peroxidase. The immunocomplex were developed by the Tyramide labelling kit (Roche) giving a fluorescent complex (in 520 nm). General methods were adapted and applied to our conditions (Morel, et al. 2001 Sambrook & Russell, 2001). After that, immunostaining was applied as described in "Immunostaining".

8. Conclusions

1. Schmidt-Lanterman Incisures and Nodes of Ranvier are pathways for ribosomes and RNAs to be related to axonal function.

2. CMT human patients' nerves showed inhomogeneous neurofilament arrangements in axons. Myelin is delaminated. Big groups of ribosomes are present near the irregular newborn axonal sprouting. Ribosomes have been found also in axoplasm.

3. The presence of *pmp22* transcript and PMP-22 protein signals in nuclear domains during myelinogenesis and in TrJ/+ adult fibers described here (Fig. 4), suggest other type of alterations. They would be, a) altered post-transcriptional regulation? and/or b) altered motor protein link, both potentially involved in pathogenesis and illness consolidation.

9. Acknowledgements

CSIC-Universidad de la República, Montevideo, Uruguay, PEDECIBA, MEyC, ANII, FIRCA-NIH. The authors especially thank Dr. Timothy De Voogd (Professor at the University of Cornell, NY, USA) for his careful reading and correction of the present manuscript.

10. References

Aguayo, AJ, Atiwell, M, Trecarten, J, Perkins, S, Bray, M. 1977. Abnormal myelination in transplanted Trembler mouse Schwann cells. Nature 265: 73-75.

Berciano, J. and Combarros, O. 2003. Hereditary Neuropathies. Current Opinion in Neurology, 16: 613-622.

Bozzola, JJ & Russell, LD, 1998. Electron Microscopy. Principles and techniques for Biologists, ISBN 0763701920. 2nd edition, Jones & Bartlett Publischers, Sudbury, Massachusetts.

Depillar ME, Tang S, Mukhopadhyay G, Shen YJ, Filbin MT. 1996.
Myelin-associated glycoprotein inhibits axonal regeneration from a variety of neurons via interaction with a sialoglycoprotein. Mol Cell Neurosci.;7(2):89-101.

Cajal, SRY. 1928. Degeneration and regeneration of the nervous system, volumenes I y II Oxford University Press London.

Cornbrooks CJ, Mithen F, Cochran JM, Bunge RP.1982.Factors affecting Schwann cell basal lamina formation in cultures of dorsal root ganglia from mice with muscular dystrophy. Brain Res. ;282(1):57-67.

Court FA, Hendriks WT, MacGillavry HD, Alvarez J, van Minnen J. 2008. Schwann cell to axon transfer of ribosomes: toward a novel understanding of the role of glia in the nervous system. J Neurosci.;28(43):11024-9.

Court FA, Midha R, Cisterna BA, Grochmal J, Shakhbazau A, Hendriks WT, Van Minnen J. 2011.Morphological evidence for a transport of ribosomes from Schwann cells to regenerating axons. Glia. 2011 Oct;59(10):1529-39. doi: 10.1002/glia.21196. Epub 2011 Jun 8.

Devaux J.J. & Scherer SS , 2005 .Altered Ion Channels in an Animal Model of Charcot-Marie-Tooth Disease Type IA, The Journal of Neuroscience, February 9, • 25(6):1470 – 1480.Fortun J, Li J, Go J, Fenstermaker A, Fletcher BS, Notterpek L. 2005- Impaired proteasome activity and accumulation of ubiquitinated substrates in a hereditary neuropathy model. J Neurochem. ;92:1531–1541.

Fortun J, Verrier JD, Go JC, Madorsky I, Dunn WA, Notterpek L. 2007.The formation of peripheral myelin protein 22 aggregates is hindered by the enhancement of autophagy and expression of cytoplasmic chaperones.Neurobiol Dis. ;25(2):252-65.

Ghabriel, MN and Allt G. 1987. Incisures of Schmidt-Lanterman, Progress in Neurobiology vol 17,25-58.

Ghabriel MN, Allt G. 1981. Incisures of Schmidt-Lanterman. Prog Neurobiol1,7(1-2):25-58.

Ghabriel MN, Allt G. 1980a. Schmidt-Lanterman incisures. II. A light and electron microscope study of remyelinating peripheral nerve fibres.Acta Neuropathol. 52(2):97-104.

Ghabriel, MN and Allt G. 1980b Schmidt-Lanterman incisures I. A light an electron microscopy study of remyelinating peripheral nerve fibres. Acta Neuropathol.52, 85-95.

Ghabriel MN, Allt G. 1979a. The role of Schmidt-Lanterman incisures in Wallerian degeneration. II. An electron microscopic study.Acta Neuropathol. 48(2):95-103.

Ghabriel, MN and Allt G. 1979b. The role of Schmidt-Lanterman ncisures in Wallerian degeneration. I. A quantitative teased fibre study. Acta Neuropathol. 48, 83-93.

Goldberg AL. 2003. Protein degradation and protection against misfolded or damaged proteins. Nature.;426(6968):895-9. Review.

Hall, SM & Williams, PL. 1970. Studies on the incisures of Schmidt and Lanterman. J. Cell Sci. 6, 767-791.

Inherited Peripheral Neuropathies Mutation Database, http://www.molgen.ua.ac.be/cmtmutations/

Henry, E.; Cowen, J.; Sidman, R. (1983) Comparison of Trembler and Trembler- J Phenotypes: varying severity of peripheral hypomyelination. Journal of Neuropathology and Experimental Neurology, 42, 688-706.

Henry EW, Sidman RL. 1983.The murine mutation trembler-J: proof of semidominant expression by use of the linked vestigial tail marker.J Neurogenet.;1(1):39-52.

Hiscoe, HB, 1947. Distribution of nodes and incisures in normal and regenerated nerve fibers. Anat. Rec 99, 447-475.

Junn E, Lee SS, Suhr UT, Mouradian MM. 2002. Parkin accumulation in aggresomes due to proteasome impairment.J Biol Chem 6;277(49):47870-7.

Khajavi M, Shiga K, Wiszniewski W, He F, Shaw CA, Yan J, Wensel TG, Snipes GJ, Lupski JR. 2007- Oral curcumin mitigates the clinical and neuropathologic phenotype of the Trembler-J mouse: a potential therapy for inherited neuropathy. Am J Hum Genet.;81(3):438-53.

Koenig E & Martin R. 1996. Cortical plaque-like structures identify ribosome-containing domains in the Mauthner cell axon. J Neurosci.;16(4):1400-11.

Koenig E, Martin R, Titmus M, & Sotelo-Silveira J. 2000. Cryptic Peripheral Ribosomal Domains Distributed Intermittently along Mammalian Myelinated Axons. The Journal of Neuroscience, November 15, 2000, *20*(22):8390–8400.

Kun A, J. C. Benech, A. Giuditta & J.R. Sotelo. 1998. Polysomes are present in the squid giant axon: an Immuno Electron Microscopy. ICEM-14, Electron Microscopy, 1998, Vol. I:825-826.

Kun, A, Otero, L., Sotelo-Silveira, J. & Sotelo, J. 2007. Ribosomal distribution in axón of mammalian myelinated fibers. J.Neuroscience Research 85:2087-2098

Li YC, Li YN, Cheng CX, Sakamoto H, Kawate T, Shimada O & Atsumi S .2005. Subsurface cisterna-lined axonal invaginations and double-walled vesicles at the axonal-myelin sheath interface. Neurosci Res.;53(3):298-303.

Li YC, Cheng CX, Li YN, Shimada O, & Atsumi S. 2005.Beyond the initial axon segment of the spinal motor axon: fasciculated microtubules and polyribosomal clusters. J Anat; 206(6):535-42.

MacKenzie ML, Ghabriel MN & Allt G. 1984. Nodes of Ranvier and Schmidt-Lanterman incisures: an in vivo lanthanum tracer study.J Neurocytol. 13(6):1043-55.–

Martin R, Fritz W & Giuditta A. 1989. Visualization of polyribosomes in the postsynaptic area of the squid giant synapse by electron spectroscopic imaging. J Neurocytol.; 18(1):11-8.

Mersiyanova IV, Perepelov AV, Polyakov AV, Sitnikov VF, Dadali EL, Oparin RB, Petrin AN & Evgrafov OV, 2000. A new variant of Charcot-Marie-Tooth disease type 2 is probably the result of a mutation in the neurofilament-light gene. Am J Hum Genet 67: 37-46.

Morel G, Cavalier A & Williams L. 2001. In situ hybridization in electron microscopy CRC Press Boca New York Washington, D.C. ISBN 0849300444, 9780849300448. Editors Morel G, Cavalier A, Williams L.

Notterpek L, Ryan MC, Tobler AR & Shooter EM. 1999. PMP-22 accumulation in aggresomes: implications for CMT1A pathology. Neurobiol Dis. ;6(5):450-60.

Notterpek L, Shooter EM & Snipes GJ. 1997. Upregulation of the endosomal-lysosomal pathway in the trembler-J neuropathy. J Neurosci.;17(11):4190-200.

Patel PI, Roa BB, Welcher AA, Schoener-Scott R, Trask BJ, Pentao L, Snipes GJ, Garcia CA, Francke U, Shooter EM, Lupski JR & Suter U. 1992.The gene for the peripheral myelin protein PMP-22 is a candidate for Charcot-Marie-Tooth disease type 1A. Nat Genet.;1(3):159-65.

Pérez-Ollé, R, Leung, CL, Liem, RKH. 2002. Effects of Charcot-Marie-Tooth linked mutation of the neurofilament light subunit on intermediate filament formation. Journal of Cell Science 115:4937-4946.

Quarles RH. 2007.Myelin-associated glycoprotein (MAG): past, present and beyond.J Neurochem.100(6):1431- 48.

Ryan TE, Patterson SD. 2002.Proteomics: drug target discovery on an industrial scale.Trends Biotechnol.;20(12 Suppl):S45-51. Review.

Robertson JD. 1958. The ultrastruture of Schmidt Lanterman clefts and related shearing defects of the myelin sheath. J. Biophis. Biochem. Cytol., 4, 39-46. 48.

Rosso G, Cal K, Canclini L, Damián JP, Ruiz P, Rodríguez H, Sotelo JR, Vazquez C, Kun A. 2010. Early phenotypical diagnoses in Trembler-J mice model. J Neurosci Methods;190(1):14-9.

Salzer JL, Brophy PJ, Peles E. 2008. Molecular Domains of Myelinated Axons in the Peripheral Nervous System. Glia 56:1532–1540

Sambrook Y, Russell DW. 2006. Molecular Cloning A laboratory manual. Third edition. Cold Spring Harbor Laboratory Press. ISBN 0879697717

Sereda M, Griffiths I, Pühlhofer A, Stewart H, Rossner MJ, Zimmerman F, Magyar JP, Schneider A, Hund E, Meinck HM, Suter U, Nave KA. 1996. A transgenic rat model of Charcot-Marie-Tooth disease. Neuron.;16(5):1049-60.

Shen YJ, DeBellard ME, Salzer JL, Roder J, Filbin MT. 1998.Myelin-associated glycoprotein in myelin and expressed by Schwann cells inhibits axonal regeneration and branching.Mol Cell Neurosci. 1998 Sep;12(1-2):79-91.

Sidman, R.; Cowen, J.; Eicher, E. 1979. Inheredit muscle and nerve diseases in mice: A tabulation with commentary. Ann NY Academy Science, 317, 497-505.

Small JR, Ghabriel MN, Allt G 1987. The development of Schmidt-Lanterman incisures: an electron microscope study.J Anat.150:277-86.

Snipes GJ, Suter U.1995. Molecular basis of common hereditary motor and sensory neuropathies in humans and in mouse models.Brain Pathol. ;5(3):233-47.

Snipes GJ, Suter U. 1995.Molecular anatomy and genetics of myelin proteins in the peripheral nervous system. J Anat.;186 (Pt 3):483-94. Review.

Sotelo JR, Kun A, Benech JC, Giuditta A, Morillas J, Benech CR.1999. Ribosomes and polyribosomes are present in the squid giant axon: an immunocytochemical study.Neuroscience.; 90(2):705-15.

Sotelo-Silveira JR, Calliari A, Kun A, Koenig E, Sotelo JR. 2006.RNA trafficking in axons.Traffic.;7(5):508-15. Review.

Suter,U. and Scherer, S. 2003, Disease mechanisms in inherited neuropathies. Nature Rev Neurosc 4:714-726.

Suter U, Moskow JJ, Welcher AA, Snipes GJ, Kosaras B, Sidman RL, Buchberg AM, Shooter EM.1992. A leucine-to-proline mutation in the putative first transmembrane domain of the 22-kDa peripheral myelin protein in the trembler-J mouse.Proc Natl Acad Sci U S A.; 15;89(10):4382-6.

Valentijn LJ, Baas F, Wolterman RA, Hoogendijk JE, van den Bosch NH, Zorn I, Gabreëls-Festen AW, de Visser M, Bolhuis PA. 1992.Identical point mutations of PMP-22 in Trembler-J mouse and Charcot-Marie-Tooth disease type 1A. Nat Genet. ;2(4):288-91.

Vallat JM, Funalot B. 2010 Charcot-Marie-Tooth (CMT) disease: an update.Med Sci (Paris). 2010 Oct;26(10):842-7.

Verhoeven K, De Jonghe P, Coen K, Verpoorten N, Auer-Grumbach M, Kwon JM, FitzPatrick D, Schmedding E, De Vriendt E, Jacobs A, Van Gerwen V, Wagner K, Hartung HP, Timmerman V. 2003. Mutations in the Small GTP-ase Late Endosomal Protein RAB7 Cause Charcot-Marie-Tooth Type 2B Neuropathy. Am J Hum Genet 72: 722-727

Waelter S, Boeddrich A, Lurz R, Scherzinger E, Lueder G, Lehrach H, Wanker EE. 2001. Accumulation of mutant huntingtin fragments in aggresome-like inclusion bodies as a result of insufficient protein degradation. Mol Biol Cell.;12(5):1393-407.

Young P, Suter U. 2003.The causes of Charcot-Marie-Tooth disease.
Cell Mol Life Sci. ;60(12):2547-60.

Zelená J. 1970.Ribosome-like particles in myelinated axons of the rat. Brain Res.; 1;24(2):359-63.

Zelená J. 1972. Ribosomes in the axoplasm of myelinated nerve fibres.Folia Morphol (Praha).;20(1):91-

Zelená J. 1972. Ribosomes in myelinated axons of dorsal root ganglia. Z Zellforsch Mikrosk Anat. 1972;124(2):217-29.

Zhao C, Takita J, Tanaka Y, Setou M, Nakagawa T, Takeda S, Yang HW, Terada S, Nakata T, Takei Y, Saito M, Tsuji S, Hayashi Y, Hirokawa N. 2001. Charcot-Marie-Tooth disease type 2A caused by mutation in a microtubule motor KIF1Bbeta. Cell, 1;105(5):587-97.

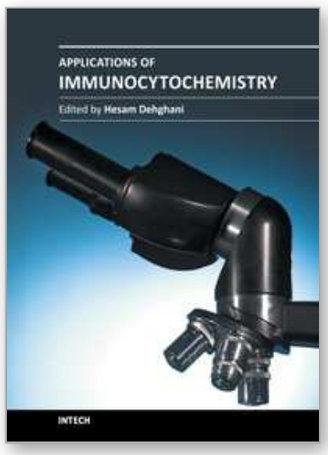

Applications of Immunocytochemistry
Edited by Dr. Hesam Dehghani

ISBN 978-953-51-0229-8
Hard cover, 320 pages
Publisher InTech
Published online 09, March, 2012
Published in print edition March, 2012

Immunocytochemistry is classically defined as a procedure to detect antigens in cellular contexts using antibodies. However, over the years many aspects of this procedure have evolved within a plethora of experimental setups. There are different ways to prepare a given specimen, different kinds of antibodies to apply, different techniques for imaging, and different methods of analyzing the data. In this book, various ways of performing each individual step of immunocytochemistry in different cellular contexts are exemplified and discussed. Applications of Immunocytochemistry offers technical and background information on different steps of immunocytochemistry and presents the application of this technique and its adaptations in cell lines, neural tissue, pancreatic tissue, sputum cells, sperm cells, preimplantation embryo, arabidopsis, fish gonads, and Leishmania.

INTECH
open science | open minds

InTech Europe
University Campus STeP Ri
Slavka Krautzeka 83/A
51000 Rijeka, Croatia
Phone: +385 (51) 770 447
Fax: +385 (51) 686 166
www.intechopen.com

InTech China
Unit 405, Office Block, Hotel Equatorial Shanghai
No.65, Yan An Road (West), Shanghai, 200040, China
中国上海市延安西路65号上海国际贵都大饭店办公楼405单元
Phone: +86-21-62489820
Fax: +86-21-62489821

IntechOpen